CHEMISTRY
A EUROPEAN JOURNAL

DOI: 10.1002/chem.200500868

VIP

Synthesis, Liquid-Crystalline Properties, and Supramolecular Nanostructures of Dendronized Poly(isocyanide)s and Their Precursors

Yanqing Tian,*[a, b] Kaori Kamata,[a, c] Hirohisa Yoshida,[a] and Tomokazu Iyoda*[a, c]

Abstract: A series of novel dendronized π-conjugated poly(isocyanide)s were synthesized successfully by using a Pd–Pt μ-ethynediyl dinuclear complex ($[ClPt\{P(C_2H_5)_3\}_2C{\equiv}CPt\{P(C_2H_5)_3\}_2Cl]$) as the initiator. The polymerizations of the dendronized monomers follow first-order kinetics, indicating that living polymerization takes place. The obtained polymers exhibit narrow polydispersities in the range of 1.03–1.20. Thermal properties of the poly(isocyanide)s as well as their isocyanide monomers and precursors with formamido (HCONH-) moieties as apexes were investigated by using differential scanning calorimetry (DSC), polarized optical microscopy (POM) and wide-angle X-ray diffraction (WAXD). Both the peripheries and the apex groups of the dendrons affect the formation of supramolecular column and/or cubic phases of the precursors and monomers. The formamido precursor forms a liquid-crystalline phase due to intermolecular hydrogen bonding. The isocyanide monomer lacks this hydrogen-bonding ability and does not display an organized mesophase. All of the rigid poly(isocyanide)s with the monodendrons exhibit columnar liquid-crystalline phases. Interestingly, cylindrical structures of a poly(isocyanide) were directly visualized by using transmission electron microscopy (TEM).

Keywords: dendrimers · liquid crystals · living polymerization · nanostructures · polymers

Introduction

The synthesis of dendronized polymers, which may also be called polymers with appendant dendrons or dendrimers with a polymer core, possessing desirable properties of the dendrimers, that is, high solubility, low intrinsic viscosity, self-assembly ability, and so forth, have caused scientific interest.[1] Such dendronized macromolecules could be prepared either by polymerization of an appropriate dendronized monomer or by appending dendrimer segments to an existing polymer.[1h] Most of the reported dendronized polymers are have flexible polymethacrylates, polystyrenes, and/or functional poly(p-phenylene)s as the backbones.[1c–e,h] Herein, we will report the synthesis and investigation of new dendronized polymers with the rigid poly(isocyanide) backbone. In this study, we have placed the emphasis on both the rigidity of the rodlike polymer backbone and the living polymerization character which allows us to build macromolecular nanostructures.

Poly(isocyanide)s are quite different from conventional polymers, such as polystyrene and polymethacrylate, and may keep a rigid helical conformation with the 4_1-type helix with a pitch of about 0.4 nm even in the racemic polymers, such as the poly(*tert*-butyl isocyanide).[2,3] Many poly(isocyanide)s with chiral and/or achiral functional and/or nonfunctional side-groups have been prepared[4] for the study of the influence of chiral groups on the helicity, for the demonstration of nonlinear dynamics of the high-order helical structures, for the elucidation of the ion-channel properties, and for direct visualization of the helical structures through microphase separation of block copolymers by atomic force microscopy (AFM) and transmission electron microscopy (TEM). As another strategy to fabricate the poly(isocyanide)-based nanostructures, we have attempted to introduce liquid crystalline (LC) properties into the rigid helical π-

[a] Dr. Y. Q. Tian, Dr. K. Kamata, Prof. H. Yoshida, Prof. T. Iyoda
Department of Applied Chemistry
Graduate School of Engineering, Tokyo Metropolitan University
1-1 Minami-Ohsawa, Hachioji, Tokyo, 192–0397 (Japan)
E-mail: yqtian@u.washington.edu
iyoda@res.titech.ac.jp

[b] Dr. Y. Q. Tian
Present address:
Materials Science and Engineering, University of Washington
Box 352120, Seattle, WA 98195-2120 (USA)
Fax: (+1) 206-543-3100

[c] Dr. K. Kamata, Prof. T. Iyoda
Present address:
Chemical Resources Laboratory, Tokyo Institute of Technology
4259 Nagatsuta, Midori-ku, Yokohama, Kanagawa 226-8503 (Japan)
Fax: (+81) 45-924-5266

conjugated poly(isocyanide)s. The combination of the helical properties and LC properties may not only result in a new class of functional materials, but also endow the poly(isocyanide)s with interesting optical and thermal properties. However, due to the rigid nature of the poly(isocyanide) backbones, only few poly(isocyanide)s were found to show the liquid crystalline properties.[5] Herein, we utilize monodendrons with long alkyl chains,[1d,e,j–m,6] which allow us to expect interesting self-assembly specific nanostructures, such as cylindrical or cubic supramolecular structures, as the peripheral groups of the poly(isocyanide) backbone. Dendron substituents on the poly(isocyanide) backbone are programmed to induce self-assembling process to give ordered nanostructures. To obtain the dendronized poly(isocyanide)s with defined molecular weights and with narrow polydispersities, we chose the living polymerization technique developed by Takahashi et al.,[7] in which the successive and multiple insertion of the isocyanide into the Pd–C bond of the Pd–Pt μ-ethynediyl dinuclear complex may produce polymers with narrow polydispersities in quantitative yields.

On the other hand, generally, compounds with the formamido (HCONH-) group and isocyano (-NC) moiety are necessary precursors and monomers for the preparation of poly(isocyanide)s. Though many papers investigated the monodendrons with different peripheries, generations, and polar groups at the apex (such as COOH, COONa, COOCs, $CO(OCH_2CH_2)_nOH$, metal cations, etc),[6,8] there is still no report describing the synthesis and liquid-crystalline properties of the monodendrons with formamido and/or isocyano units as the polar apex groups.

In the article, we will describe the preparative procedure, the thermal properties, and the supramolecular structures of the dendronized poly(isocyanide)s, including their corresponding monodendrons with formamido and isocyano groups.

Results and Discussion

Synthesis and characterization: Isocyanide monomers for the liquid-crystalline (LC)-dendronized poly(isocyanide)s were derived from esterification of the known monodendrons bearing hydroxyl groups (**1** and **2**)[6] with 4-formamidobenzoic acid to give new monodendrons **3** and **4**

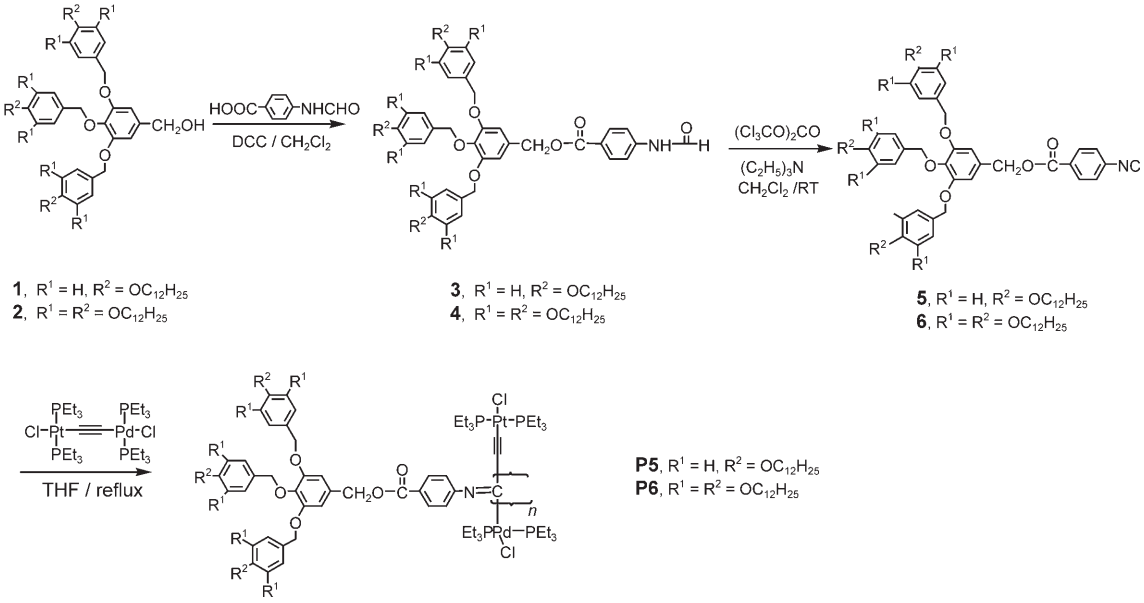

Scheme 1.

Table 1. Experimental conditions and properties of the synthesized poly(isocyanide)s.

Runs	Monomer	$[\mathbf{M}]_0/[\mathbf{I}]_0$	Obtained polymers	Polymerization time [h]	Conversion [%]	Yield [%]	$M_{n,GPC}$[b]	$M_{n,calcd}$[c]	M_w/M_n[d]
1	**5**	100	**P5a**	2	23	~10	10900	26300	1.03
2	**5**	100	**P5b**	22	92	77	23200	102800	1.06
3	**5**	170	**P5c**	72	98	90	33600	186000	1.20
4	**6**	10	**P6a**	48	88	70	10100	20800	1.05
5	**6**	20	**P6b**	57	81	59	11700	36300	1.03
6	**6**	100	–[a]	336	22	–[a]	–	49600	–

[a] Not isolated. [b] Number average molecular weight (M_n) determined by GPC. [c] M_n calculated based on the feed ratio and conversions. [d] Polydispersity determined by GPC.

(Scheme 1) as precursors for the dendronized isocyanide monomers. After dehydration of the formamido groups in **3** and **4** with (trichloromethyl)carbonate (triphosgene), monodendrons **5** and **6** as monomers were afforded in yields of ~70%. Polymerizations of the monomers (Table 1) were carried out in THF at 75°C. Purities of the monodendrons and polymers were guaranteed by using IR and ^{1}H NMR spectroscopy, gel permeation chromatography (GPC), and/or elemental analysis.

The IR spectra of the purified polymers showed no signal corresponding to the isocyano moiety. Weak broad bands from the formed imino groups constituting the polymer backbone were observed at approximately 1645 cm^{-1}, confirming the formation of the poly(isocyanide)s' backbone. A very weak band of −C≡C− at 2085 cm^{-1} was detected in the resulting poly(isocyanide)s, implying that the insertion polymerization proceeded successfully and the structure of the initiator remains in the polymer; this in turn leads to further living polymerization.[7] The ^{1}H NMR spectra of the polymers just show very broad resonance in both the aromatic and aliphatic chain regions. All the polymers gave unimodal GPC profiles with narrow polydispersities from 1.03 to 1.20 (Figure 1 and Table 1).

Kinetic of the polymerization: Figure 2 shows the kinetic plots of the polymerization procedures of monodendron **5** with the feed ratio of $[\mathbf{5}]_0/[\mathbf{I}]_0 = 100$ and of monodendron **6** with the feed ratio of $[\mathbf{6}]_0/[\mathbf{I}]_0 = 20$. A linear dependence of $\ln([\mathbf{M}]_0/[\mathbf{M}])$ on the polymerization reaction time was observed, demonstrating that the polymerizations of the dendronized monomers follow first-order kinetics. Taking the $[\mathbf{5}]_0/[\mathbf{I}]_0 = 100$ system as an example, molecular weights increase with increasing monomer conversion. The polydispersities are in the narrow range of 1.03–1.06 (Figure 3). This behavior confirms the living character of the polymerization under the present conditions. The molecular weights determined by GPC are much lower than the molecular weights calculated according to the feed ratio and conversions. The significant discrepancy is probably due to the quite different hydrodynamic volumes of the dendronized polymers from those of the linear polystyrenes that are used for the calibration materials for GPC columns.

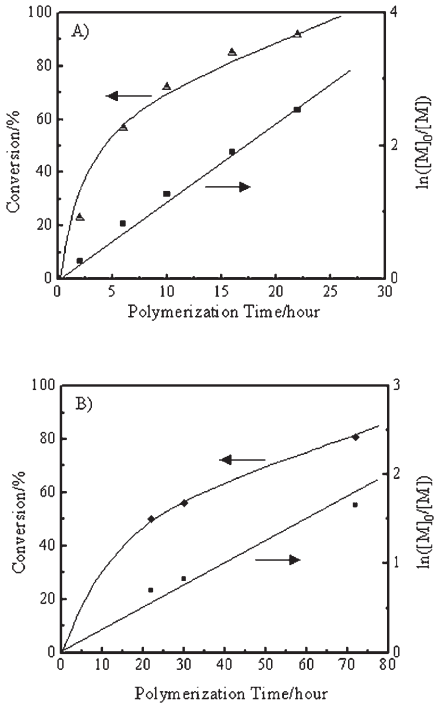

Figure 2. The first-order kinetic plots of the polymerization of A) monomer **5** with the feed ratio ($[\mathbf{M}]_0/[\mathbf{I}]_0$) of 100 and B) **6** with the feed ratio of 20 by the μ-ethynediyl Pd–Pt dinuclear complex as the initiator in THF heated under reflux.

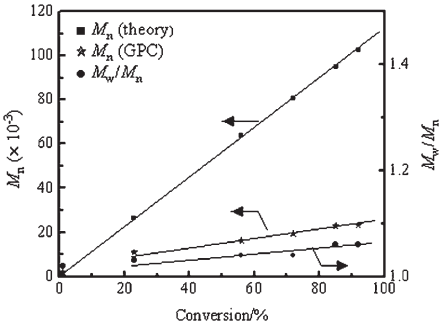

Figure 3. Dependence of molecular weigh (M_n) and polydispersity (M_w/M_n) on the conversion of the monodendric monomer **5**.

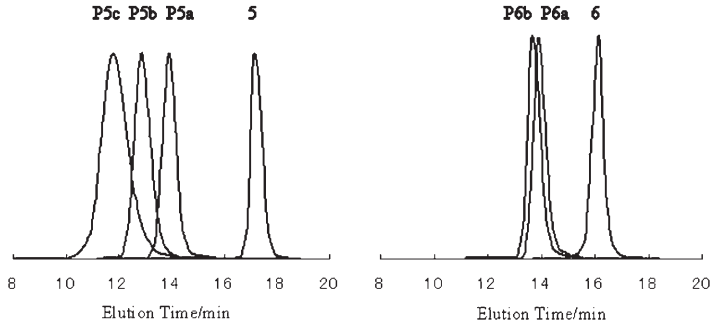

Figure 1. The GPC curves of monomer **5**; polymers **P5a**, **P5b**, and **P5c**; monomer **6**; and polymers **P6a**, and **P6b**.

Polymerization rates of the two monodendrons of **5** and **6** are quite different. The polymerization of the large monodendron **6** was much slower than that of the small monodendron **5**, which may be attributed to their different peripheries resulting in their different weight fractions of the isocyano groups in the monomers. Polymers with high polymerization degrees (e.g., DP = 100) with the monodendron **6** as the monomer could not be obtained. After one week polymerization, the conversion of a polymerization of **6**, expected for DP = 100, was just about 22%. However, the polymerization of **5** with high DP proceeded well. The conversion of the polymerization of **5** for DP = 170 reached 98% only within three days.

Thermal properties of the monodendrons—precursors and monomers: Figure 4 gives the differential scanning calorimetry (DSC) curves of the monodendron **3**. The first heating of **3** shows two sharp endothermic peaks at 69 and 79 °C, corresponding to its crystal–crystal (Cr_1–Cr_2) and crystal–isotropic-liquid (Cr–I, or melting) transitions. The first cooling of this compound shows a small exothermic peak at 77 °C corresponding to an isotropic-liquid–mesophase (I–M) transition and a broad baseline shift at about 33 °C corresponding to a mesophase–glass transition (M–g). On the second heating, the monodendron **3** undergoes a cold crystallization at about 25 °C followed by complex melting processes until the isotropic transition at 77 °C. The second cooling cycle gives the same result as the first one. Upon cooling from the isotropic state, clear fan-shaped textures (Figure 5) were observed by polarized optical microscopy (POM), indicating the possible hexagonal columnar phase (Col_h),[9] which was further confirmed by using wide-angle X-ray diffraction (WAXD).

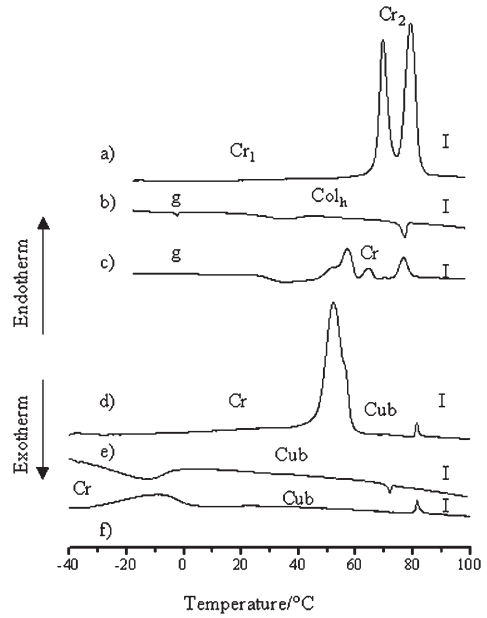

Figure 4. DSC curves of the monodendron **3** and **4**. a) first heating of **3**; b) first cooling of **3**; c) second heating of **3**; d) first heating of **4**; e) first cooling of **4**; f) second heating of **4**.

Figure 5. Typical texture of the monodendron **3** at 60 °C on cooling. Magnification: ×200.

The first heating of monodendron **4** shows a sharp endothermic peak at 53 °C corresponding to the crystal–mesophase (Cr–M) transition and a weak endothermic peak at 82 °C corresponding to the M–I transition, as illustrated in Figure 4. On cooling, a much wider mesophase temperature range was observed. Under POM, no birefringence was observed, suggesting that the mesophase is a cubic (Cub) phase.

The DSC curves of the monodendrons with isocyano group, **5** and **6**, exhibit only a melting peak on heating and a crystalline peak on cooling with a big enthalpy as given in Table 2.

Figure 6 illustrates the wide-angle X-ray diffractograms of the monodendrons **3** and **4**. For the monodendron **3**, the X-ray diffractogram at 60 °C on cooling shows a sharp (100) and two weak (110) and (200) Bragg reflections in small-angle region with a lattice spacing ratio of $d_{100}:d_{110}:d_{200}=1/(1/3^{1/2})/(1/4^{1/2})$ indicates that the mesophase is a hexagonal columnar phase (Col_h) with a lattice of $a=50.1$ Å.[10] On cooling to room temperature, the X-ray diffractogram changes slightly. The ratio of the lattice spacing still follows the order of $d_{100}:d_{110}:d_{200}=1/(1/3^{1/2})/(1/4^{1/2})$, suggesting the ordered columnar structures were frozen in the glassy state. The absence of a sharp reflection in the wide-angle region in its columnar mesophase and existence of a diffuse halo caused by the liquidlike arrangement of the alkyl side chains suggest an irregular (disordered) arrangement of the mole-

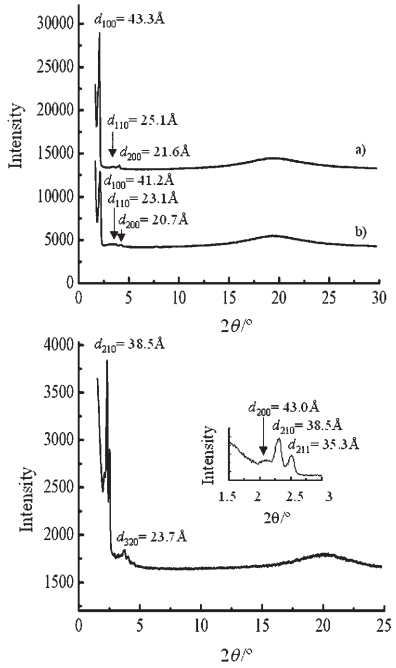

Figure 6. he X-ray diffractograms of **3** (top) measured at 60 °C (a) and 25 °C (b) on cooling, and **4** (bottom) measured at 25 °C on cooling.

Table 2. The phase behaviors of the monodendrons and their polymers.

	Phase-transition temperatures [°C][a]	Measured lattice spacings and proposed indexes
3	Cr_1 69 (39.2) Cr_2 79 (56.3) I[b]	$d_{100}=43.3$ Å; $d_{110}=25.1$ Å; $d_{200}=21.6$ Å (60 °C, cooling)
	I 77 (−3.4) Col_h 33 (−3.8) g[c]	$d_{100}=41.2$ Å; $d_{110}=23.1$ Å; $d_{200}=20.7$ Å (25 °C, cooling)
4	I 72 (−0.8) Cub −12 (−20.8) Cr[c]	$d_{200}=43.0$ Å; $d_{210}=38.5$ Å; $d_{211}=35.3$ Å; $d_{320}=23.7$ Å (25 °C, cooling)
	Cr −10 (18.1) Cub 81 (1.3) I[d]	
5	I 37 (−141.3) Cr[c]	
	Cr 67 (168.7) I[d]	
6	I 30 (−172.2) Cr[c]	
	Cr 62 (178.6) I[d]	
P5a	Cr ~36[e] (91.8) M ~260 decomp[f]	$d=39.5$ Å (30 °C, after annealing at 100 °C)
P5b	Cr 43 (40.3) Col_h ~260 decomp[f]	$d_{100}=39.4$ Å; $d_{110}=22.3$ Å (100 °C)
P5c	Cr 45 (50.6) M ~260 decomp[f]	$d=39.6$ Å (100 °C)
P6a	Cr −12 (25.9) M ~260 decomp[f]	$d=36.7$ Å (30 °C, after annealing at 100 °C)
P6b	Cr −12 (29.2) M ~260 decomp[f]	$d=36.6$ Å (80 °C)

[a] Enthalpies [kJ mol^{-1}] are given in parentheses. [b] On the first heating cycle. [c] On the first cooling cycle. [d] On the second heating cycle. [e] Broad transition. [f] Decomposition on heating. Cr: crystalline phase; M: Mesophase, possibly columnar phase; Col_h: hexagonal columnar phase; Cub: cubic phase; I: isotropic phase; g: glass state.

cules within the parallel aligned columns independent of the two-dimensional lattice. For the monodendron **4**, four Bragg reflections corresponding to the (200), (210), (211), and (320) with a lattice spacing ratio $d_{200}:d_{210}:d_{211}:d_{320}=(1/4^{1/2})/(1/5^{1/2})/(1/6^{1/2})/(1/13^{1/2})$ were observed, indicating the cubic mesophase with a lattice parameter of $a=80.5$ Å.[11]

The phase-transition temperatures and transition enthalpies obtained from the above thermal investigations are summarized in Table 2. The phase behavior depends on not only the peripheries, but also the apex groups. The two monodendrons with formamido apex groups, **3** and **4**, form the column or cubic phases, respectively, which are dependent on their peripheries. The two monodendrons with isocyano apex groups, **5** and **6**, do not exhibit liquid-crystalline properties regardless of their peripheries. Comparison of the isotropic transition temperatures of **3** and **4** with their related dehydrated monodendrons, **5** and **6**, it can be seen that the isotropic transition temperature of each monodendron with formamido group is about 10 or 15 °C higher than that of its related monodendron with an isocyano group. This observation suggests the formamido group may stabilize the mesophase. Considering their structural difference, we think the different thermal properties might possibly be due to intermolecular hydrogen bonding through the formamido apexes.

To confirm the above consideration, typical IR spectra of the monodendrons **3** and **5** were measured and are illustrated in Figure 7. For both the two compounds, the ester carbonyl vibration at 1717 cm^{-1} was observed. Two formamido carbonyl vibrations of **3** at 1683 and 1678 cm^{-1} were observed, confirming the existence of intermolecular hydrogen bonding between the formamido groups through the s-*cis* interaction (dimer, 1683 cm^{-1}) and the s-*trans* interaction (polymer, the predominating state for the amide, 1678 cm^{-1})[12] as illustrated in Scheme 2. Due to the dehydration of the formamido group, the intermolecular hydrogen bonding of **3** is broken and the resulting isocyanide vibration of **5** appears at 2120 cm^{-1}. Therefore, the results from IR spectra clearly indicate that intermolecular hydrogen bonding does exist in the formamido moiety containing precursors. Further study is in progress by using temperature-dependent IR and Raman spectra for more detailed understandings of the relationship between the intermolecular hydrogen bonding and thermal properties.

Thermal properties of the polymers: Thermal properties of the polymers were first examined by means of thermogravimetric analysis, revealing that all of the polymers are stable up to

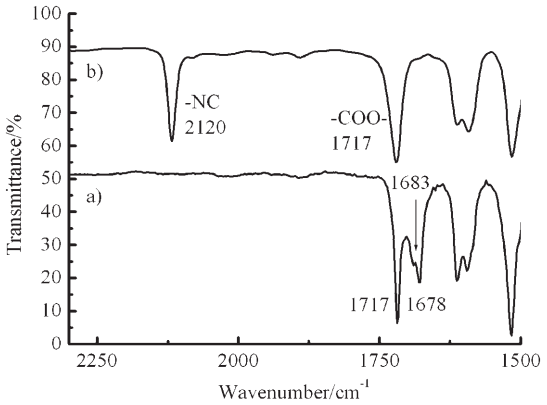

Figure 7. The IR spectra of a) the precursor monodendron **3** and b) its dehydrated monomer **5**.

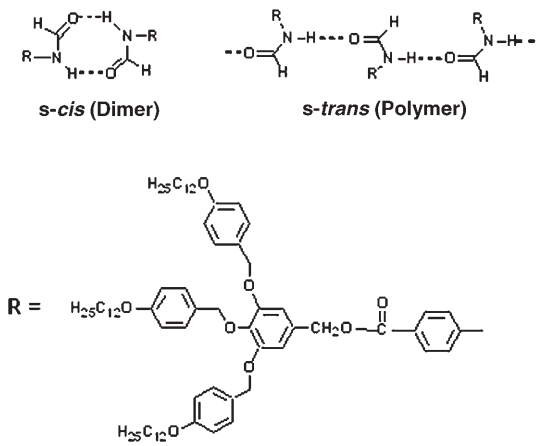

Scheme 2. The possible intermolecular hydrogen bonding between the formamido groups.

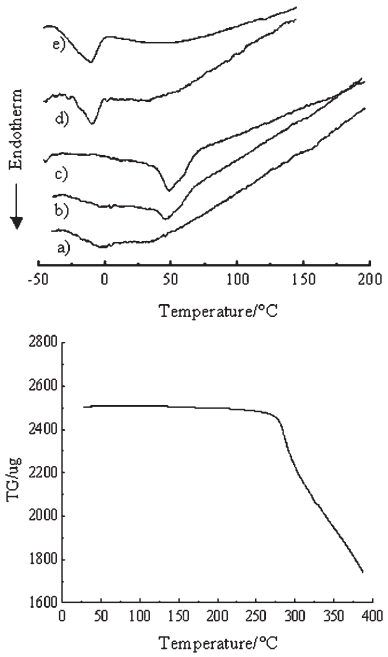

Figure 8. Top: DSC curves of a) **P5a**, b) **P5b**, c) **P5c**, d) **P6a**, and e) **P6b** for the heating process. Bottom: TG-DTA curve of **P5b**.

260 °C. The DSC profile of polymers of **5** (**P5**) showed a reversible phase transition at about 40–50 °C (Figure 8) depending on their molecular weights, but no further phase transitions were observed before their decomposition. The DSC results for polymers of **6** (**P6**) showed a reversible transition at about −12 °C. No isotropization transition was observed for any of the polymers before their decompositions, as confirmed by temperature-dependent wide-angle X-ray diffraction and polarized microscopy. The thermal properties are summarized in Table 2. Under polarized optical microscopy, very strong birefringence was observed in the LC phase of **P5**. The textures are not characteristic of columnar phases or smectic phases, and are difficult to identify. No birefringence was observed for **P6**. The lack of typical textures of the polymers with monodendrons has already been reported by Percec's group.[1d,f,j] Therefore, X-ray diffraction analysis (Figure 9) becomes a powerful tool to gain more information about the mesophormic structures. All of the polymers show a sharp peak in the small angle region and a broad hollow in the wide-angle region of $2\theta \approx 20°$, indicating formation of their mesophases. Especially, the diffractogram of **P5b** shows a sharp diffraction peak at 3.94 nm (d_{100}) and a broad peak at 2.23 nm (d_{110}), strongly confirming its hexagonal columnar phase (Col_h). According to the 4_1-helical structure of the polymer backbone, the monodendrons in the side-group might generate a supramolecular columnar structure with a diameter of 4.70 nm (calculated by Chem 3D). The determined diameters (diameter $= 2\langle d_{100}\rangle/3^{1/2}$) of the columns from the X-ray diffraction measurements are 4.60 nm for **P5** and 4.30 nm for **P6**; these values are in general accordance with the calculated diameter of the column by Chem 3D (4.70 nm). Therefore, we may deduce that each of the polymers forms a columnar mesophase. The above results show that through the introduction of the flexible monodendrons into the rigid poly(isocyanide)s, LC properties, especially the hexagonal columnar LC phase, can be realized successfully.

Morphologies of the polymer P5b: Very interestingly, cylindrical structures (Figure 10) were directly viewed under TEM by using thin films of **P5b** after annealing in its columnar phase. The film was prepared by spreading about 5 μL of 1 wt% solution of **P5b** in toluene on a water surface. The thickness of the thin film was estimated to be about 50–100 nm. The films were annealed at 100 °C for 1 h in order to get the ordered structures. Small cylinders parallel to the surface with the average diameter of 4.7 nm, periodicity of 5.8 nm, and length of 18.7 nm (calculated using 100 cylinders with parallel orientation) were observed. The small cylinders found in defined areas, for example, area A in Figure 10, are tilted or perpendicular to the substrate. The different contrast reflects the different thickness of the film. The cylinders of the dendronized poly(isocyanide)s ob-

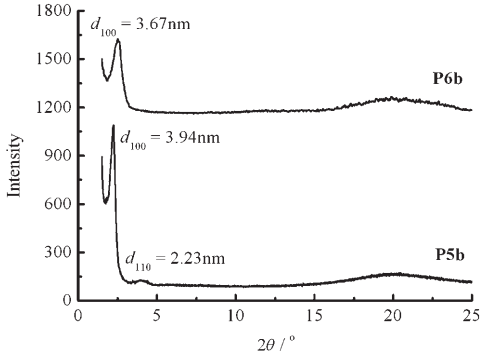

Figure 9. Wide-angle X-ray diffractograms of the polymer **P5b** and **P6b**.

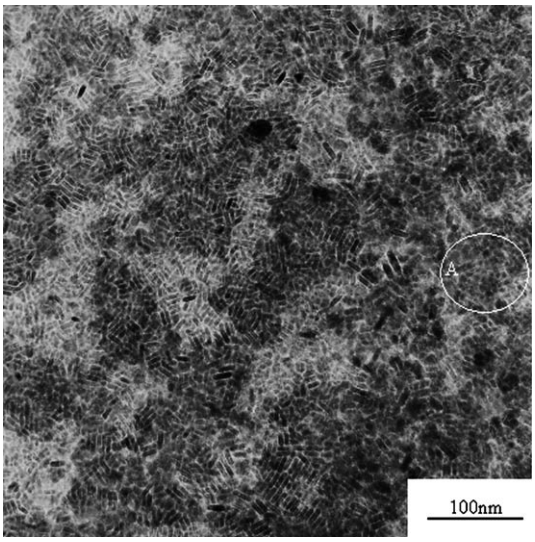

Figure 10. TEM image of the thin film of **P5b**.

served under TEM are possibly arranged as single molecules. X-ray diffraction shows the d_{100} of **P5b** is 3.94 nm, resulting in the diameter of the column is 4.60 nm (diameter = $2<d_{100}>/3^{1/2}$), which is very close to the 4.7 nm observed by TEM and the calculated value by using Chem 3D. This observation might be compared with the morphologies of linear polymethacrylates and/or polystyrenes with the similar monodendrons,[13] showing the richness of the nanostructures of the dendronized polymers. Further investigations will be addressed with the controlling of the morphologies through the adjustment of the film thickness, degree of polymerization, and even the rigidity and helicity of the backbones.

Conclusion

We reported the synthesis, liquid-crystalline properties, and supramolecular nanostructures of novel dendronized poly(isocyanide)s with their related precursors and monomers. Narrow polydispersities of the polymers were obtained using the Pd–Pt μ-ethynediyl dinuclear complex ([Cl{$P(C_2H_5)_3$}$_2$Pd≡Pt{$P(C_2H_5)_3$}$_2$Cl]) as the initiator. The polymerizations follow first-order kinetics, even though the molecular weights of the dendronized monomers are higher than 1000. Through the introduction of flexible monodendrons into the rigid poly(isocyanide)s, liquid-crystalline properties, especially the hexagonal columnar liquid-crystalline properties, are realized successfully. This provides an efficient route for endowing liquid-crystalline properties and supramolecular columnar structures on the extreme rigid poly(isocyanide)s. The cylindrical supramolecular structures of the poly(isocyanide)s were also clearly visualized using TEM.

Experimental Section

Characterization: ^{1}H NMR spectra were measured by using a JEOL 270 instrument spectrometer operating at 270 MHz with TMS internal standard as a reference for chemical shifts. FT-IR spectra were recorded on a Bio-Rad FTS 3000 spectrophotometer. All of the FT-IR measurements were performed in KBr pallet.

Molecular weights of the polymers were determined by using a JASCO 860 GPC (Japan Spectroscopic Co., Ltd.) system coupled with a UV detector, with reference to a series of standard polystyrenes as calibration with THF as eluent.

Thermal behavior was determined by using a SII Extra 6000 DSC system (Seiko Instruments Inc.) at a scanning rate of $\pm 5\,^{\circ}C\,min^{-1}$ under nitrogen. Liquid-crystalline textures were observed under a Nikon Microphot-UFX polarized optical microscopy (POM) with a Mettler FP-82 hot stage and a FP-80 central processor. Wide-angle X-ray diffraction (WAXD) was measured on a MAC Science MPX 3 X-ray diffractometer equipped with a thermal controller Model 5310.

Transmission electron microscopy (TEM, JEOL 1200 EXII) experiments were carried out at an acceleration voltage of 200 kV. TEM samples were prepared by: 1) spreading 1 wt% solutions of the sample in solutions onto water surface, 2) waiting for about 10 min until the complete evaporation of toluene and formation of uniform thin polymer films on water surface, 3) transferring the thin films onto a copper TEM grid with carbon supporting film, 4) drying the specimens at room temperature under vacuum overnight followed by annealing at 100 °C for 1 h, and 5) staining samples by using 2 wt% OsO_4 vapor for 5 min to enhance the contrast for the TEM observation.

Materials: Monodendrons **1** and **2**, and 4-formamidobenzoic acid were prepared according to the known procedures.[5,8b] The Pd–Pt μ-ethynediyl complex ([Cl{$P(C_2H_5)_3$}$_2$PdC≡CPt{$P(C_2H_5)_3$}$_2$Cl] Scheme 1) as the initiator for polymerization was prepared according to the literature.[14] THF was used as the polymerization solvent and was dehydrated by heating to reflux over sodium and then distillation under nitrogen. The other chemical reagents and solvents were commercially available and used without further purification.

Preparation of 3: 4-Formamidobenzoic acid (1.65 g, 10 mmol), **1** (9.79 g, 10 mmol), and catalytic amount of 4-*N*,*N*′-dimethylaminopyridine were dissolved in methylene chloride (150 mL) and cooled to 0–5 °C. Dicyclohexyl carbodiimide (3.09 g, 15 mmol) in methylene chloride (50 mL) was added dropwise in under stirring at 0 °C. After 12 h, the precipitate was filtered, and the solvent was removed under reduced pressure. Then the residue was purified by silica column chromatography by using chloroform/ethyl acetate as the eluent. A white product (8.1 g) with the yield of 72% was obtained after recrystallization from ethanol. ^{1}H NMR (270 MHz, $CDCl_3$, 25 °C, TMS): $\delta = 8.86$ (d, $J = 13$ Hz, 0.4H; HCO in *trans*), 8.41 (s, 0.6H; HCO in *cis*), 8.02 (d, $J = 8.9$ Hz, 2H; phenyl proton, H_m to NH), 7.60 (d, $J = 8.9$ Hz, 1.2H; phenyl proton, H_o to NH), 7.29 (d, $J = 7.8$ Hz, 6H; phenyl proton, H_m to $OC_{12}H_{25}$), 7.11 (d, $J = 7.8$ Hz, 0.8H; phenyl proton, H_o to NH), 6.85 (d, $J = 7.8$ Hz, 4H; phenyl proton, H_o to $OC_{12}H_{25}$), 6.78 (d, $J = 7.8$ Hz, 2H; phenyl proton, H_o to $OC_{12}H_{25}$), 6.71 (s, 2H; phenyl proton, H_o to CH_2OCO), 5.22 (s, 2H; CH_2O), 5.02 (s, 4H; CH_2O), 4.94 (s, 2H; CH_2O), 3.93 (m, 6H; CH_2O), 1.83–1.26 (m, 60H; $(CH_2)_{10}$), 0.84 ppm (t, $J = 6.5$ Hz, 9H; CH_3); FT-IR (KBr pellet): $\tilde{\nu} = 1718$ (C=O ester), 1679, and 1683 cm^{-1} (C=O amide); elemental analysis calcd (%) for $C_{72}H_{103}NO_9$ (1126.59): C 76.76, H 9.22, N 1.24; found: C 76.63, H 9.44, N 1.27.

Preparation of 4: This compound was synthesized from **2** by using a procedure similar to that described for **3**. Yield: 63%; ^{1}H NMR (270 MHz, $CDCl_3$, 25 °C, TMS): $\delta = 8.86$ (d, $J = 13$ Hz, 0.4H; HCO in *trans*), 8.35 (s, 0.6H; HCO in *cis*), 7.89 (m, 2H; phenyl proton, H_m to NH), 7.80 (d, $J = 8.9$ Hz, 1.3H; phenyl proton, H_o to NH), 7.55 (d, $J = 8.9$ Hz, 0.7H; phenyl proton, H_o to NH), 7.41 (s, 0.4H; NH in *trans*), 7.06 (d, $J = 7.8$ Hz, 0.6H; NH in *cis*), 6.63 (m, 2H; phenyl proton), 6.56 (m, 6H; phenyl proton), 5.13 (s, 2H; CH_2O), 4.92 (m, 6H; CH_2O), 3.83 (m, 18H; CH_2O), 1.83–1.26 (m, 180H; $(CH_2)_{10}$), 0.85 ppm (t, $J = 6.5$ Hz, 27H; CH_3); FT-IR (KBr pellet): $\tilde{\nu} = 1718$ (C=O ester) and 1679 cm^{-1} (C=O amide); elemental analysis calcd (%) for $C_{114}H_{247}NO_{15}$ (2232.50): C 77.47, H 11.15, N 0.63; found: C 77.32, H 11.47, N 0.62.

Preparation of 5: Triphosgene (0.24 g, 1 mmol) in methylene chloride (5 mL) was added slowly into a mixture of **3** (1.126 g, 1 mmol) and triethylamine (0.4 mL, 3 mmol) in methylene chloride (10 mL) at 0–5 °C. Two hours later, aqueous $NaHCO_3$ (5 wt%, 10 mL) was added to the mixture. The organic layer was separated, washed with brine, and dried by using anhydrous Na_2SO_4. After the solvent was removed under reduced pressure, the crude product was purified by column chromatography with methylene chloride as the eluent. A white solid was obtained (yield: 0.70 g, 70%). ^{1}H NMR (270 MHz, $CDCl_3$, 25 °C, TMS): $\delta = 8.06$ (d, $J = 8.6$ Hz, 2H; phenyl proton, H_o to $COOCH_2$), 7.47 (d, $J = 8.6$ Hz, 2H; phenyl proton, H_m to $COOCH_2$), 7.29 (m, 6H; phenyl proton, H_m to $OC_{12}H_{25}$), 6.88 (d, $J = 8.6$ Hz, 4H; phenyl proton, H_o to $OC_{12}H_{25}$), 6.76 (d, $J = 8.6$ Hz, 2H; phenyl proton, H_o to $OC_{12}H_{25}$), 6.65 (s, 2H; phenyl proton, H_o to CH_2OCO), 5.22 (s, 2H; CH_2O), 5.02 (s, 4H; CH_2O), 4.94 (s, 2H; CH_2O), 3.93 (m, 6H; CH_2O), 1.83–1.26 (m, 60H; $(CH_2)_{10}$), 0.84 ppm (t, $J = 6.5$ Hz, 9H; CH_3); FT-IR (KBr pellet): $\tilde{\nu} = 2120$ (−NC), 1719 cm^{-1} (C=O ester); elemental analysis calcd (%) for $C_{72}H_{101}NO_8$ (1108.57): C 78.01, H 9.18, N 1.26; found: C 77.87, H 8.97, N 1.22.

Preparation of 6: This compound was synthesized from **4** by using a procedure similar to that described for **5**. Yield: 67%; ^{1}H NMR (270 MHz, $CDCl_3$, 25 °C, TMS): $\delta = 8.00$ (d, $J = 8.6$ Hz, 2H; phenyl proton, H_m to −NC), 7.48 (d, $J = 8.6$ Hz, 2H; phenyl proton, H_o to −NC), 6.67 (m, 8H; phenyl proton, $H_{o,m}$ to OCH_2), 5.22 (s, 2H; CH_2O), 5.00 (m, 6H; CH_2O),

3.88 (m, 18H; CH_2O), 1.80–1.10 (m, 180H; $(CH_2)_{10}$), 0.88 ppm (t, J= 6.5 Hz, 27H; CH_3); FT-IR (KBr pellet): $\tilde{\nu}$=2119 (−NC), 1718 cm^{-1} (C=O ester); elemental analysis calcd (%) for $C_{114}H_{245}NO_{14}$ (2214.48): C 78.10, H 11.15, N 0.63; found: C 77.91, H 10.86, N 0.68.

Polymerization: All of the polymerizations were carried out in THF under reflux as shown in Table 1. An example of the synthesis of **P5b** is described in detail.

A mixture of the Pd–Pt μ-ethynediyl complex (4.35 mg, 0.005 mmol) as the initiator (**I**) and the monodendron **5** (554.3 mg, 0.5 mmol) was degassed under vacuum for 30 min at room temperature, then THF (20 mL) was added under nitrogen. The polymerization was carried out at 75°C. During the polymerization process, 5 μL of the solution was taken out at a specific intervals by using micro-syringe to determine the conversions. The conversion was calculated according to the integration areas of the GPC curves of the formed polymer ($A_{polymer}$) and non-polymerized monomer ($A_{monomer}$) by using Equation (1).

$$\text{Conversion} = A_{\text{polymer}/}(A_{\text{polymer}} + A_{\text{monomer}}) \quad (1)$$

After the solution was heated under refluxing for 22 h, the conversion was determined to be 92%. The solution was cooled down to room temperature and then the THF was removed under vacuum. The residue was purified by preparative GPC with $CHCl_3$ as eluent in order to remove the trace amount of nonpolymerized monomer to afford pure pale yellow polymer. Yield: 77% (430 mg); FT-IR (KBr pellet): $\tilde{\nu}$=2080 (−C≡C− in the main-chain), 1718 (C=O ester in the side-group), 1653 cm^{-1} (−N=C= in the backbone). $M_{n,GPC}$=23200, M_w/M_n=1.06. $M_{n,calcd}$=102800 [Eq. (2)].

$$M_{n,calcd} = [\mathbf{M}]_0/[\mathbf{I}]_0 \times \text{conversion} \times 1108 + 869 \quad (2)$$

In Equation (2) 1108 and 869 are the molecular weights of the monomer and initiator, respectively; the $[\mathbf{M}]_0/[\mathbf{I}]_0$ is the feed ratio of the monomer to initiator. Elemental analysis calcd (%) for $M_{n,calcd}$=102800: C 77.48, H 9.06, N 1.25; found: C 77.12, H 9.35, N 1.01.

Acknowledgements

This work was partially supported by a Grant-in-Aid from the Ministry of Education, Culture, Sports, Science, and Technology (MEXT) of the Japanese Government. We thank Prof. Shigetoshi Takahashi, Prof. Kiyotaka Onitsuka, and Dr. Fumie Takei in Osaka University for their kind supply of the Pd–Pt dinuclear complex. Y.-Q.T. thanks Japan Society for the Promotion Science for a Postdoctoral Fellowship and financial supports from MEXT.

[1] a) T. H. Mourey, S. R. Turner, M. Rubinstein, J. M. J. Fréchet, C. J. Hawker, K. L. Wooley, *Macromolecules* **1992**, *25*, 2401; b) L. J. Shu, A. Schäfer, A. D. Schlüter, *Macromolecules* **2000**, *33*, 4321; c) G. M. Stewart, M. A. Fox, *Chem. Mater.* **1998**, *10*, 860; d) V. Percec, C. H. Ann, W. D. Cho, A. M. Jamieson, J. Kim, T. Leman, M. Schmidt, M. Gerle, M. Moller, S. A. Prokhorova, S. S. Sheiko, S. Z. D. Cheng, A. Zhang, G. Ungar, D. J. P. Yeardley, *J. Am. Chem. Soc.* **1998**, *120*, 8619; e) V. Percec, D. Schlueter, *Macromolecules* **1997**, *30*, 5783; f) V. Percec, C. H. Ann, B. Barboiu, *J. Am. Chem. Soc.* **1997**, *119*, 12978; g) Z. S. Bo, A. D. Schlüter, *Chem. Eur. J.* **2000**, *6*, 3235; h) A. D. Schlüter, P. R. Jürgen, *Angew. Chem.* **2000**, *112*, 860; *Angew. Chem. Int. Ed.* **2000**, *39*, 864, and references therein; i) V, Percec, M. Glodde, T. K. Bera, Y. Miura, I. Shiyanovskaya, K. D. Singer, V. S. K. Balagurusamy, P. A. Heiney, I. Schnell, A. Rapp, H. W. Spiess, S. D. Husdon, H. Duan, *Nature* **2002**, *419*, 384; j) V. Percec, C. H. Ann, G. Unger, D. J. P. Yeardley, M. Moller, S. S. Sheiko, *Nature* **1998** *391*, 161; k) V. Percec, A. E. Dulcey, V. S. K. Balagurusamy, Y. Miura, J. Smidrkal, M. Peterca, S. Nummelin, U. Edlund, S. D. Hudson, P. A. Heiney, H. Duan, S. N. Magonov, S. A. Vinogradov, *Nature* **2004**, *430*, 764; l) G. Ungar, Y. S. Liu, X. B. Zeng, V. Percec, W. D. Cho, *Science* **2003**, *299*, 1208; m) X. B. Zeng, G. Ungar, Y. S. Liu, V. Percec, A. E. Dulcey, J. K. Hobbs, *Nature* **2004**, *428*, 157; n) A. F. Zhang, L. Okrasa, T. Pakula, A, D. Schlüter, *J. Am. Chem. Soc.* **2004**, *126*, 6658.

[2] a) F. Millich, *Chem. Rev.* **1972**, *72*, 101; b) F. Millich, *Macromol. Rev.* **1980**, *15*, 207.

[3] a) R. J. M. Nolte, A. J. M. van Beijnen, W. Drenth, *J. Am. Chem. Soc.* **1974**, *96*, 5932; b) A. J. M. van Beijnen, R. J. M. Nolte, W. Drenth, *Recl. Trav. Chim. Pays-Bas* **1980**, *99*, 121; c) A. J. M. van Beijnen, R. J. M. Nolte, W. Drenth, A. N. F. Hezemans, *Tetrahedron* **1976**, *32*, 2017.

[4] a) T. J. Deming, B. M. Novak, *J. Am. Chem. Soc.* **1993**, *115*, 9101; b) T. J. Deming, B. M. Novak, *Macromolecules* **1991**, *24*, 6043; c) M. F. M. Roks, R. J. M. Nolte, *Macromolecules* **1992**, *25*, 5398; d) B. Hong, M. A. Fox, *Macromolecules* **1994**, *27*, 5311; e) J. P. Chen, J. P. Gao, Z. Y. Wang, *Polym. Int.* **1997**, *44*, 83; f) N. Ohshiro, A. Shimizu, R. Okumura, F. Takei, K. Onitsuka, S. Takahashi, *Chem. Lett.* **2000**, 786; g) F. Takei, K. Kanai, K. Onitsuka, S. Takahashi, *Chem. Eur. J.* **2000**, *6*, 983; h) M. Kauranen, T. Verbiest, C. Boutton, M. N. Teerenstra, K. Clays, A. J. Schouten, R. J. M. Nolte, A. Persoons, *Science* **270**, *1995*, 966; i) D. B. Amabilino, E. Ramos, J. L. Serrano, J. Vaciana, *Adv. Mater.* **1998**, *10*, 1001; j) J. J. L. M. Cornelissen, M. Fischer, N. A. Sommerdijk, R. J. M. Nolte, *Science* **1998**, *280*, 1427; k) R. J. M. Nolte, *Chem. Soc. Rev.* **1994**, *23*, 11; l) D. B. Amabilino, E. Ramos, J. L. Serrano, T. Sierra, J. Veciana, *J. Am. Chem. Soc.* **1998**, *120*, 9126; m) Y. Q. Tian, Y. Li, T. Iyoda, *J. Polym. Sci. A* **2003**, *41*, 1871.

[5] C. A. van Walree, J. F. van der Pol, J. W. Zwikker, *Recl. Trav. Chim. Pays-Bas* **1990**, *109*, 561.

[6] a) V. S. K. Balagurusamy, G. Ungar, V. Percec, G. Johansson, *J. Am. Chem. Soc.* **1997**, *119*, 1539, and references therein; b) V. Percec, W.-D. Cho, G. Ungar, D. J. P. Yeardley, *J. Am. Chem. Soc.* **2001**, *123*, 1302; c) V. Percec, B. Barboiu, C. Grigoras, T. K. Bera, *J. Am. Chem. Soc.* **2003**, *125*, 6503; d) V. Percec, G. Johansson, J. Heck, G. Ungar, S. V. Batty, *J. Chem. Soc. Perkin Trans. 1* **1993**, 1411; e) V. Percec, J. Heck, D. Tomazos, F. Falkenberg, H. Blackwell, G. Ungar, *J. Chem. Soc. Perkin Trans. 1* **1993**, 2799.

[7] a) K. Onitsuka, T. Joh, S. Takahashi, *Angew. Chem.* **1992**, *104*, 893; *Angew. Chem. Int. Ed. Eng.* **1992**, *31*, 851; b) K. Onitsuka, F. Yanai, T. Takei, T. Joh, S. Takahashi, *Angew. Chem.* **1996**, *108*, 1634; *Angew. Chem. Int. Ed. Eng.* **1996**, *35*, 1554.

[8] a) G. Ungar, V. Percec, M. N. Holerca, G. Johansson, J. A. Heck, *Chem. Eur. J.* **2000**, *6*, 1258; b) V. Percec, W. D. Cho, G. Ungar, D. J. P. Yeardley, *Angew. Chem.* **2000**, *112*, 1661; *Angew. Chem. Int. Ed.* **2000**, *39*, 1598, and references there in; c) V. Percec, D. Schlueter, G. Ungar, S. Z. D. Cheng, A. Zhang, *Macromolecules* **1998**, *31*, 1745.

[9] C. Destrade, P. Foucher, H. Gasparoux, H. T. Nguyen, A. M. Levelut, J. Malthete, *Mol. Cryst. Liq. Cryst.* **1984**, *106*, 121.

[10] Hexagonal columnar lattice parameter $a=2\langle d_{100}\rangle/\sqrt{3}$, in which, $\langle d_{100}\rangle=(d_{100}+\sqrt{3}d_{110}+\sqrt{42}d_{200})/3$.

[11] Cubic lattice parameter $a=\langle d_{200}\rangle$, in which $\langle d_{200}\rangle=(d_{200}+\sqrt{5}d_{210}+\sqrt{6}d_{211}+\sqrt{13}d_{320})/4$.

[12] *Spectrometic Identification of Organic Compounds* (Eds.: R. M. Silverstein, F. X. Webster), Wiley, 6th ed., **1997**, p. 101.

[13] a) S. A. Prokhorova, S. S. Sheiko, M. Moller, C. H. Ann, V. Percec, *Macromol. Rapid Commun.* **1998**, *19*, 359; b) S. A. Prokhorova, S. S. Sheiko, C. H. Ann, V. Percec, M. Moller, *Macromolecules* **1999**, *32*, 2654; c) W. Stocker, B. L. Schürmann, J. P. Rabe, S. Förster, P. Lindner, I. Neubert, A. D. Schlüter, *Adv. Mater.* **1998**, *10*, 793.

[14] S. Takahashi, Y. Ohyama, E. Murata, K. Sonogashira, N. Hagihara, *J. Polym. Sci. Polym. Chem. Ed.* **1980**, *18*, 349.

Received: July 22, 2005
Published online: September 27, 2005

